



Phytotoxicity of Silver Nanoparticles with Different Surface Properties on Monocots and Dicots Model Plants

Ewelina Matras¹ · Anna Gorczyca¹ · Ewa Pocięcha² · Sebastian Wojciech Przemieniecki³ · Magdalena Oćwieja⁴

Received: 13 October 2021 / Accepted: 4 January 2022 / Published online: 13 January 2022
© The Author(s) 2022

Abstract

The aim of the research was to evaluate the effect of three types of silver nanoparticles (AgNPs) with different physicochemical properties and silver ions delivered in the form of silver nitrate (AgNO_3) at the concentration of 50 mg L^{-1} on germination and initial growth of monocots (common wheat, sorghum) and dicots (garden cress, white mustard). The AgNPs were prepared using trisodium citrate (TCSB-AgNPs), tannic acid (TA-AgNPs), and cysteamine hydrochloride (CHSB-AgNPs). They exhibited comparable shape, size distribution, and an average size equal to $15 \pm 3 \text{ nm}$ which was confirmed with the use of transmission electron microscopy. The electrokinetic characteristics revealed that CHSB-AgNPs have positive, whereas TCSB-AgNPs and TA-AgNPs negative surface charge. First, toxicity of the silver compounds was assessed using the Phytotestkit test. Next, after transferring seedlings to pots, shoot length, leaf surface, shoot dry mass, electrolyte leakage measurement, and photosystem II (PSII) efficiency were determined. AgNPs and silver ions delivered in the form of AgNO_3 reduced root and shoots length of common wheat, sorghum, and garden cress; leaves surface of garden cress and white mustard; and shoots dry mass of white mustard. The positively charged CHSB-AgNPs and silver ions delivered in the form of AgNO_3 showed the greatest inhibition effect. Moreover, silver ions and positively charged CHSB-AgNPs were more toxic to PSII of model plants than negatively charged TCSB-AgNPs and TA-AgNPs. AgNPs impact differed in the case of monocots and dicots, but the size of the changes was not significant, so it concerned individual parameters. The results revealed the interaction strength, which was generally similar in all tested plants, i.e., increasing negative effect in sequence TCSB-AgNPs < TA-AgNPs < silver ions delivered in the form of AgNO_3 < CHSB-AgNPs.

Keywords Silver nanoparticles · Surface properties · Charge · Model plants · Phytotoxicity

Abbreviations

NPs	Nanoparticles
AgNO_3	Silver nitrate
AgNPs	Silver nanoparticles
TCSB-AgNPs	AgNPs prepared with the use of sodium borohydride and trisodium citrate
TA-AgNPs	AgNPs prepared with the use of tannic acid
CHSB-AgNPs	AgNPs prepared with the use of sodium borohydride and cysteamine hydrochloride

1 Introduction

Nanomaterials are used in various sectors of the economy due to their unique properties. They are used, among others, in the textile, food, medicine, pharmacology, biotechnology, electronics, engineering, and energy industries, and recently, they are also gaining popularity in agriculture and environmental protection (Gorczyca et al. 2021; Hu and Xianyu 2021; Khan et al. 2019; Naidu et al. 2015; Shukla et al. 2019). World production of nanomaterials amounts to 11 million tonnes with a total value of around EUR 20 billion (European Commission 2019). Despite the great benefits, their abuse and lack of knowledge about interactions with biological systems can pose a serious threat to the proper functioning of ecosystems (Du et al. 2018; Tangaa et al. 2016).

Plants are the basis of most ecosystems. As primary producers, they represent a potential transport pathway for NPs

✉ Ewelina Matras
ewelina.matras@urk.edu.pl

Extended author information available on the last page of the article

to higher trophic levels (biomagnification) (Rajput et al. 2020). One of the most common nanomaterials is AgNPs. Many scientists have shown that AgNPs cause a number of negative effects on plants by inducing cytotoxicity, genotoxicity, an immune response, and even cell death (Akter et al. 2017; Cvjetko et al. 2018; Malandrakis et al. 2021; Pinsino et al. 2020; Pradas Del Real et al. 2017; Tripathi et al. 2017; Yan and Chen 2019). Plants in response to metal stress often show disturbances in vital functions in terms of morphological, physiological, and biochemical changes. Photosynthesis is a key metabolic process that determines the proper growth and development of plants (Heyneke and Fernie 2018). Depending on the different photosynthetic pathways of C3 and C4 plants, their photosynthetic reaction and defense mechanisms in the presence of NPs are different (Bai et al. 2021). In general, C4 plants show 50% better photosynthetic efficiency than most C3 plants (Kajala et al. 2011). The most important difference between these plants is in the carbon dioxide (CO₂) binding pathway. In the case of plants, C3—CO₂ is fixed by the Calvin cycle in mesophilic cells, and the rate-limiting factor is the Rubisco enzyme, as it reacts not only with CO₂ but also with oxygen (O₂) leading to photorespiration (Parry et al. 2013). In turn, plants C4 bind CO₂ to a 3-carbon compound, resulting in a stable 4-carbon product. The CO₂ enrichment mechanism allows C4 plants to transpire at a lower rate compared to C3 plants, but they are characterized by a higher efficiency of water use, thus reducing the accumulation and transport of pollutants and metals (Evans 2013; Ye et al. 2020). Moreover, C4 plants are characterized by a more effective antioxidant defense under abiotic stress conditions, which may indicate that C4 plants are more tolerant to the toxic effects of NPs than C3 plants (Nayyar and Gupta 2006; Uzilday et al. 2014; Zhao et al. 2020).

The toxicity of NPs can also vary depending on the plant form. Formerly flowering plants were divided into two groups: monocotyledons and dicotyledons, while the current system groups angiosperms into clades (Angiosperm Phylogeny Group et al. 2016; Yang et al. 2020). Monocots have an embryo with one cotyledon and a fibrous root system, while dicotyledons-taproot and an embryo with two cotyledons (Chen et al. 2018; Sabelli 2012). The bundles in monocot plants are scattered across the entire width of the stem and closed, whereas bundles in dicots are arranged in a ring (concentric) and have the form of an open bundle with cambium, which allows the stem to grow in thickness (Scarpella and Meijer 2004). Stomata are important for leaf gas exchange and transpiration for both forms. The stomata in monocotyledonous plants are evenly distributed in parallel rows and occur in the same number on both sides of the leaf. In turn, the stomata of dicots are randomly distributed in the lower epidermis of leaves. They are not exposed to excessive evaporation as the underside of the leaves is not

exposed to direct sunlight (Han and Torii 2016; Hepworth et al. 2018). Moreover, both forms of plants differ in terms of the morphology of leaves and flowers (Conklin et al. 2019; Linh et al. 2018; Soltis and Soltis 2016).

The mechanism of action of AgNPs has not been clearly established. It is hypothesized that it is closely related to the released silver ions from the AgNPs surface which enhances their toxicity (Pradas Del Real et al. 2017; Vinković et al. 2017). There are also opinions that AgNPs themselves also have toxic properties (Geisler-Lee et al. 2013; Wang et al. 2020; Yin et al. 2011).

The toxicity profile of NPs is largely determined by their size, shape, and surface chemistry (Oćwieja et al. 2017; Silva et al. 2014; Sukhanova et al. 2018). Smaller particles are believed to be more toxic as they have a larger active surface that can interact with the surroundings (Scherer et al. 2019; Yan and Chen 2019; Yin et al. 2011). In addition, small particles can more easily penetrate the interior of plant cells and damage them. The pores in the plant cell wall are usually small in diameter, about 3–20 nm, which makes it easier for only selected particles to pass through the pores (Chichiricò and Poma 2015; Koushik et al. 2019). Despite this, studies have been reported showing that larger NPs can enlarge the pores in the cell wall and thus penetrate the interior (Navarro et al. 2008).

Another factor influencing the bioactivity of NPs are the stabilizers adsorbed on their surface. Depending on the type of stabilization, their molecules can cause a number of chemical reactions and physical processes taking place on their surfaces (Akter et al. 2017; Kujda et al. 2015). First of all, they can influence the processes of oxidative dissolution of AgNPs and thus mask or enhance their toxicity in relation to the toxicity of silver ions at the same concentration (Jiang et al. 2009; Oćwieja et al. 2014). In addition, properly selected stabilizers enable the control of the electrokinetic properties of NPs and, consequently, attractive or off-putting interactions with charged living cells (Tolaymat et al. 2010).

Interpretation of the interaction of nanochemicals on organisms requires a detailed knowledge of all important features of NPs. Indication of the exact characteristics of NPs is omitted in studies assessing the toxicity of a given type of NPs to various organisms, including plants. The form of the plant is also an important element in assessing the toxicity of NPs. There are still no studies at this level of detail that would provide an answer to the topic of what is the response of plants – globally the most important autotrophic organisms entering trophic chains first and having great importance for the state of the environment – to NPs whose release into the environment is constantly growing dynamically. Risk assessment caused by the presence of nanomaterials in the environment is particularly important in the case of newly synthesized products, especially those with commercial potential (Cox et al. 2017).

The aim of the research was to compare the differences in the impact of AgNPs produced by chemical reduction against the background of silver ions delivered in the form of AgNO₃ on selected species of model plants. The AgNPs used in the study were characterized by various physico-chemical properties such as surface properties and charge but quite similar size and shape. The seeds of four model plant species were treated – two monocots (one C3 and one C4 photosynthetic pathways) and two dicots. The evaluation was performed on the initial growth of these plants, i.e., germination, biometry, cell wall damage, and photosynthetic efficiency. It was assumed whether the contact of plant seeds with AgNPs and silver ions delivered in the form of AgNO₃ disturbs the initial growth of plants with different morphological and physiological properties.

2 Materials and Methods

2.1 Reagents

Silver nitrate, trisodium citrate dihydrate, sodium borohydride, tannic acid, cysteamine hydrochloride, and ammonia solution (25%) were purchased from Sigma Aldrich. These chemicals were of analytical grade and used without further purification. Ultrapure water used for preparation of the AgNP suspensions was produced by Milli-Q Elix & Simplicity 185 purification system (Millipore SA Molsheim, France).

2.2 Seeds of Model Plants

The seeds of spring common wheat (*Triticum aestivum* L.) cv. Tybalt were obtained from the Research Centre for Cultivar Testing in Slupia Wielka (Poland). The seeds of sorghum (*Sorghum bicolor* L. Moench), garden cress (*Lepidium sativum* L.), and white mustard (*Sinapis alba* L.) were purchased from Tigret Company (Poland) as original material parts of the Phytotestkit test.

2.3 Synthesis of AgNPs

Citrate-silver nanoparticles (TCSB-AgNPs) were obtained according to the modified Lee and Meisel (1982) protocol using sodium borohydride (SB) and trisodium citrate (TC) as a reducing and stabilizing agent, respectively. Briefly, 200 mL of 8 mM freshly prepared SB aqueous solution was mixed with 200 mL of 20 mM TC solution. Then, while stirring, the 100 mL of 1 mM AgNO₃ solution was added dropwise into the reduction mixture for 20 min. The reaction was allowed to proceed, while being continually stirred, under ambient conditions for 90 min.

Tannic acid-silver nanoparticles (TA-AgNPs) were synthesized by a reduction of formed silver amino complexes with tannic acid (TA) molecules. For this purpose, 40 mL of 0.5 mM aqueous solution of TA was introduced to 320 mL of 11 mM AgNO₃ solution. After, the dynamic stirring 30 μL of 25 wt % ammonia solution was introduced to the obtained reaction mixture. The stirring was continued for another 30 min.

Cysteamine-silver nanoparticles (CHSB-AgNPs) were prepared by a functionalization of negatively charged AgNPs synthesized with the use of sodium borohydride (SB) with cysteamine hydrochloride (CH) under acidic conditions (Barbasz et al. 2017). Briefly, 2.5 mL of 5 mM freshly prepared aqueous solution of SB was added dropwise to 200 mL of 2.5 mM aqueous solution of AgNO₃. After 10 min of vigorous stirring at room temperature, 10 mL of 1.5 mM of freshly prepared aqueous solution of CH was added dropwise to the newly formed AgNPs. The mixing was continued for additional 60 min.

After the preparation procedure, the AgNP suspension was introduced to an Amicon® filtration cell (model 8400) equipped with membranes made of regenerated cellulose of a nominal molecular weight limit of 100 kDa. The purification process was conducted under ambient conditions (at the temperature of 25 °C, atmospheric pressure). The filtration cell was placed on magnetic stirrer, and in this way, gentle mixing of the suspension during the purification procedure was ensured. Each suspension was washed using MilliQ-water. The progress in the purification procedure was monitored via conductivity measurements. For this purpose, the conductivity of collected effluents (usually every 50 mL of collected effluent) was determined using CPC-505 pH meter/conductometer (Elmetron) equipped with a conductometric sensor EC-60. The purification process was finished when the effluent conductivity attained value of 3.2–5.7 μS/cm and pH stabilized ca. 5.8–6.2. It is worth mentioning that the volume of each stock suspension (after the purification procedure) was 2–3 times smaller than the volume of reaction mixture.

2.4 Characteristics of AgNPs

The procedure of determination of mass concentration of AgNP in the stock suspension is based on the results of density measurement of AgNP suspension and a dispersive medium (effluent without AgNPs) which are conducted with the use of densitometer providing relatively precise of measurements of 5×10^{-6} (Oćwieja et al. 2011). In the experiments, a DMA500 M densitometer (Anton Paar) was used for the determination of density of stock AgNP suspension (ρ_s) and the effluent solution (ρ_e) collected during the purification procedure. Then, the weight fraction of Ag in the stock suspensions was calculated from the formula:

$$w = \frac{\rho_p(\rho_s - \rho_e)}{\rho_s(\rho_p - \rho_e)} \quad (1)$$

where $\rho_p = 10.40 \text{ g cm}^{-3}$ is the specific density of AgNPs.

The optical properties of AgNP suspension was evaluated applying a UV-2600 spectrometer (Shimadzu). The stability, polydispersity (polydispersity index PdI), and electrokinetic properties of AgNPs in the suspensions of controlled concentration, pH, ionic strength, and temperature were determined using Zetasizer Nano ZS instrument (Malvern) according to the procedures described in detail previously (Gorczyca et al. 2022). The morphology of AgNPs was determined using micrographs recorded with the use of a JEOL JSM-7500F electron microscope working in the transmission mode (TEM). The size distribution and average size of each type of AgNPs were established analyzing no less than 1000 nanoparticles in a MultiScan software (Computer scanning system) (Gorczyca et al. 2022). The oxidative dissolution of AgNPs was assessed measuring the concentration of leached silver ions in the suspensions of controlled pH, ionic strength, temperature, and concentration of dissolved oxygen (DO) after given periods of time. For this purpose, the suspensions of AgNP concentration equal to 10 mg L^{-1} were filtered using a regenerated cellulose membrane (Millipore, nominal molecular weight limit 30 kDa) in order to separate the AgNPs from released silver ions. The concentrations of silver ions in the effluents were measured using a PinAAcle 900Z atomic absorption spectrometer (AAS) (Perkin Elmer).

2.5 Test Phytotestkit

The toxicity of AgNPs and silver ions delivered in the form of AgNO_3 was determined using the Phytotestkit test. The mass concentration of AgNPs in the applied suspensions as well as silver ions delivered in the form of AgNO_3 was equal to 50 mg L^{-1} . The Phytotestkit test was performed according to the manufacturer's recommended procedure (MicroBioTests Inc., Belgium) (Phytotoxkit 2004). The test is based on measuring the germination and root growth of the plants after 3 days of exposure to the AgNPs and silver ions delivered in the form of AgNO_3 in comparison to the germination and growth of these plants in the control (sterile tap water). The test was carried out on plates consisting of two parts: lower and upper, which allow direct observation of seed germination and seedling growth. The growth of roots occurs in the lower part, while the growth of shoots of the plants takes place in the top part. The lower chamber of the test plate was filled with a foam pad and a thick filter paper, which was then soaked in 20 mL of the analyzed silver compounds. Thereafter, the lower part of the test plates was covered with a black paper filter, and the seeds of the

test plants were sown at 10 per plate. The prepared plates were incubated in a horizontal position at $25 \text{ }^\circ\text{C}$ in the dark for 72 h. After this time, pictures were taken with a digital camera, and then, using the image analysis program Image J, the number of germinated seeds was determined, and the length of the roots was measured. The entire experiment was carried out in triplicate for each analyzed object. The seed germination capacity was determined by calculating the seed germination percentage (G):

$$G = \frac{\text{number of germinating seeds}}{\text{total number of seeds}} \cdot 100 \quad (2)$$

In turn, the percentage inhibition of germination (IG) and root growth (IR) was calculated according to the following formula:

$$IG \text{ or } IR = \frac{AB}{A} \cdot 100\% \quad (3)$$

where A is the average seed germination or root length in the control and B is average seed germination or root length treated with AgNPs and silver ions delivered in the form of AgNO_3 .

A germination index (GI) was calculated according to the following formula:

$$GI = \frac{GsLs}{GcLc} \cdot 100\% \quad (4)$$

where Gs and Ls are the seed germination (percent) and root elongation (mm) of the plants after the exposure on the AgNPs and silver ions delivered in the form of AgNO_3 , and Gc and Lc are the values detected for the untreated seeds/plants.

2.6 Pot Experiment

After 7 days from the establishment of the experiment, the germinated seeds were transferred to plastic pots filled with perlite and placed in a growth chamber with controlled conditions: light $200 \mu\text{mol m}^{-2} \text{ s}^{-1}$ PPFD (AGRO Philips sodium lamps) and temperature $20 \text{ }^\circ\text{C}$, photoperiod 12/12 h day/night. The plants were monitored daily and moistened water as needed. The plants were grown for 14 days. After this time, the morphological and physiological analysis of the seedlings of the tested plants was performed. The length of the shoots, the surface of the leaves, and the fresh and dry mass of the shoots were analyzed. The Leaf Area Meter CI-202 (CID Bio-Science (USA)) was used to measure the assimilation area of leaves. The fresh weight of the wheat seedlings was weighed on a laboratory scale, while the dry weight of the seedlings was weighted after drying the plants at $70 \text{ }^\circ\text{C}$ for 72 h in a laboratory dryer (Memmert GmbH + Co.KG, Germany). On the basis

of fresh and dry matter, the percentage dry matter content in seedlings of the tested plants was calculated.

2.7 Measurements of Electrolyte Leakage

The leave pieces of plants collected from each treatment were placed into vials containing 10 cm³ of ultrapure water (one piece per vial). They were shaken (100 rpm) at 20 °C. After 24 h, electrical conductivity (E1) was measured using a CI 317 conductometer (Elmetron, Poland). Then, in order to cause maximum damage, the fragments of plants flooded with water in the tubes were transferred to the freezer at – 80 °C for 24 h. After that, the vials were shaken for 24 h, and the conductivity was measured again. The obtained values represented total ion content (E2) in the leave pieces. Membrane permeability was expressed as the percentage of total electrolyte leakage (EL) (Eich et al. 2000). All measurements were performed for 10 biological replicates.

2.8 Measurements of Photosystem II Efficiency

The efficiency of photosystem II was measured using a plant efficiency analyzer (PEA; Hansatech Ltd., King's Lynn, UK) with an excitation light intensity of 3 mmol m⁻² s⁻¹. The measurements were carried out after a 30 min adaptation of leaves to darkness. The following parameters of PSII efficiency including phenomenological or specific energy fluxes and activities as well as JIP test were calculated based on Strasser et al. (2000): ABS, energy absorption; TR₀, energy flux for trapping; ET₀, energy flux for transport of electrons; and DI₀, dissipation of energy. These values were expressed per CS (cross section of the sample) or RC (reaction center). Moreover, RC/CS₀, active PS II reaction center per exited cross section; φE₀, quantum yield for electron transport; ψ₀, probability of electron transport; and OEC, oxygen-evolving complex were calculated. The measurements of PSII efficiency were done on the youngest fully developed leaves in 10 replications per treatment. The measurements of PSII efficiency were performed only for common wheat, sorghum, and white mustard because the surface of the garden cress leaf was too small to insert a clip.

2.9 Statistical Analyses

The data was tested for normality of distribution (Shapiro–Wilk test) firstly and homogeneity of variance (Levene's test), and then, the differences between results were determined by analysis of variance (ANOVA) (at a significance determined by Duncan's test) or Kruskal–Wallis test (at a significance determined by Dunn's test with Bonferroni correction). Results were shown as boxplot divided into quartiles with median and mean. The relationships between observations were determined by principal

component analysis (PCA) based on Pearson correlation matrix and agglomerative hierarchical clustering (AHC) based on Bray and Curtis dissimilarity with Wards method. To construct the Pearson correlation matrix for PCA, we used the centralization of the results for each trait according to the formula: ((result-mean)/standard deviation). Lengths between variables were computed by principal coordinate analysis (PCoA) using transformed data (according to the above formula). PCoA for variants was performed using 2 dimensions, because the introduction of the 3rd dimension did not significantly affect the distribution of the observed variants. The explanation value of the variance for F1 and F2 was 98.9%, while F3 was only 0.5% with an eigenvalue of 0.001. The results were processed statistically and interpreted graphically in XLSTAT program (Addinsoft, UK).

3 Results

3.1 Characteristics of AgNPs

The mass concentration of AgNPs in the stock suspensions determined based on the density measurements varied between 123 (TCSB-AgNPs) and 189 mg L⁻¹ (TA-AgNPs). Nevertheless, for the biological studies, the stock suspensions were diluted to the concentration of 50 mg L⁻¹ using MilliQ water. It is worth mentioning that the aqueous solution of AgNO₃ was also prepared in a manner allowing to maintain silver ion concentration equal to 50 mg L⁻¹.

Each AgNP suspension was characterized by intense yellow color. The spectra of AgNP suspension used in the experiments are shown in Fig. 1a. The values of plasmon absorption maxima obtained for each type of AgNPs are collected in Table S1. The microscopic analysis conducted using TEM showed that independently on the preparation procedure, the AgNPs were spherical and uniform. Typical TEM micrographs and the size distribution of AgNPs are presented in Fig. 1b–d. It was established that the average size of TCSB-AgNPs and TA-AgNPs was equal to 15 ± 4 nm and 17 ± 5 nm, respectively. CHSB-AgNPs were the smallest among the AgNPs. Their average size attained value of 12 ± 4 nm.

The stability and electrokinetic properties of AgNPs were also carefully determined in the suspensions which were used in the biological experiments. The measurements of diffusion coefficients and electrophoretic mobility were conducted every 24 h for 7 days and additionally after 30 days. Knowing the values of AgNP diffusion coefficients (Table S1), the hydrodynamic diameters were calculated using the Stokes–Einstein equation. In turn, the values of electrophoretic mobility were applied to determine the zeta potential of AgNPs based on the Henry's equation. The values of these parameters determined for the initial time of

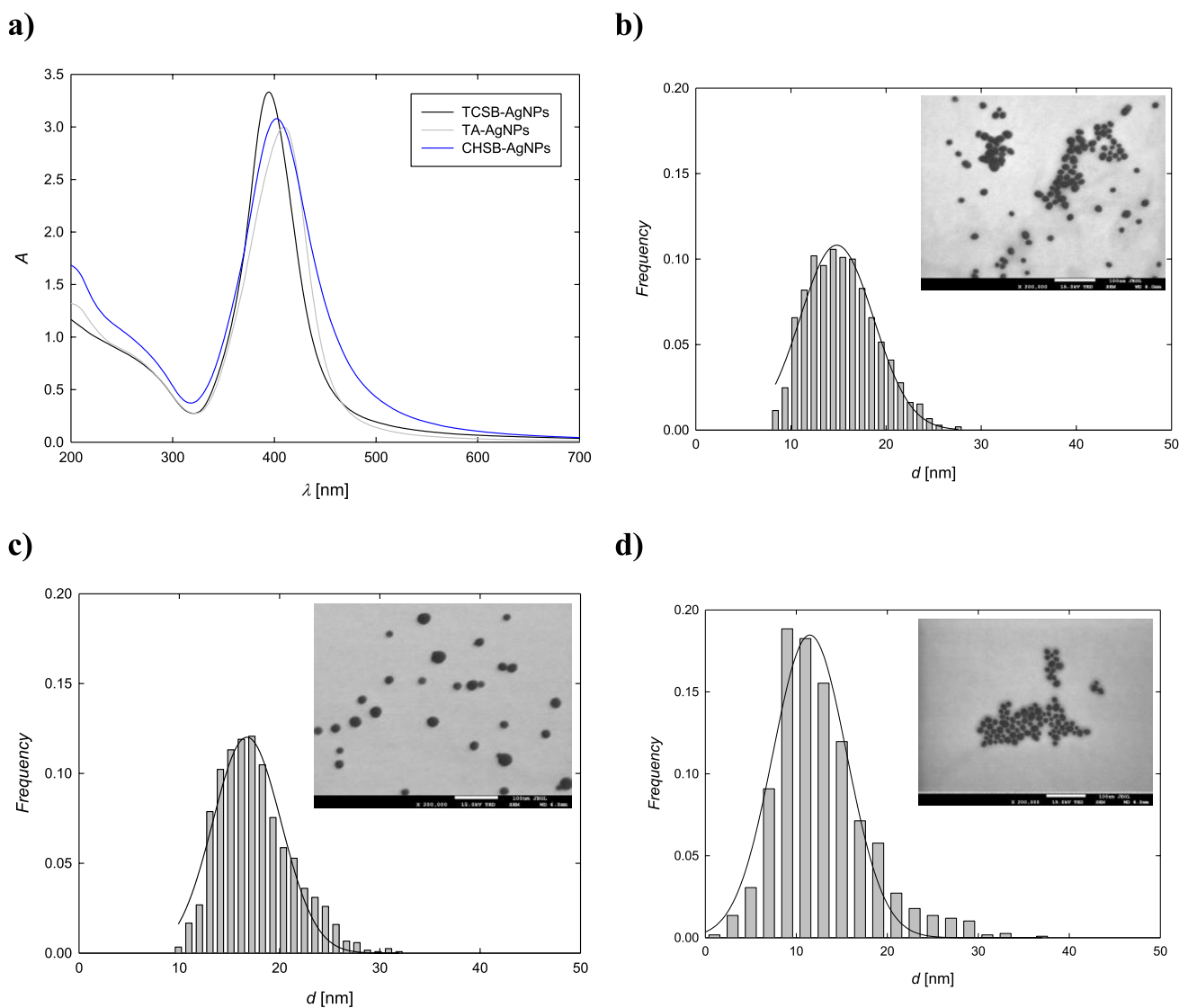


Fig. 1 Extinction spectra of AgNPs suspension (a) and size distribution of TCSB-AgNPs (b), TA-AgNPs (c), CHSB-AgNPs (d). The insets present typical TEM micrographs of AgNPs (scale bare 100 nm, magnification $\times 200\,000$)

studies are collected in Table S1, whereas the dependencies of hydrodynamic diameter and zeta potential on time are presented in Fig. 2. Generally, it was established that the values of hydrodynamic diameter of AgNPs determined by dynamic light scattering technique (DLS) were in accordance with the values obtained from the TEM imaging. The AgNPs dispersed in the aqueous suspensions of pH 5.8–6.2, at temperature of 20 °C, were highly stable, and their hydrodynamic values remained unchanged (Fig. 2a). Moreover, it was found that CHSB-AgNPs were the most monodisperse and their polydispersity index was equal to 0.26 (Table S1). The measurements of electrophoretic mobility revealed that TCSB-AgNPs and TA-AgNPs were negatively charged, whereas CHSB-AgNPs were characterized by positive surface charge (Table S1). The values of zeta potential of both

negatively charged types of AgNPs were comparable and equal to -66 ± 3 mV and -64 ± 3 mV. It was found that the zeta potential of these AgNPs was stable during the whole time period of biological experiments (Fig. 2). Similar dependence was observed for positively charged CHSB-AgNPs which zeta potential was equal to $+58 \pm 2$ mV.

The investigations of AgNP effluents conducted with the use of AAS revealed that these solutions obtained via the ultrafiltration method were free of silver ions at the beginning of the experiments. The AAS measurements carried out for the effluents collected after 7 days of the suspension storage at the temperature of 20 °C and DO concentration of 6.9–7.2 mg L⁻¹ showed that the silver ion content increased significantly for each type of AgNP suspensions. The concentration of silver ions present in the AgNP suspensions as

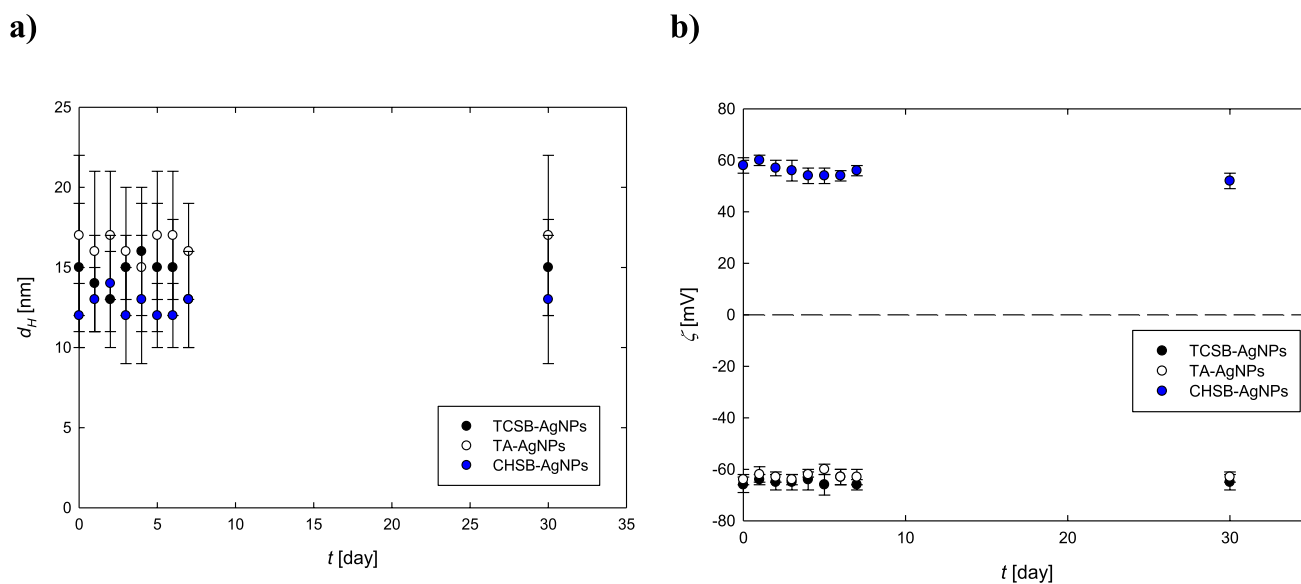


Fig. 2 The dependence of hydrodynamic diameter (a) and zeta potential (b) of AgNPs on time. The measurement conditions: concentration of AgNPs 50 mg L^{-1} , pH 5.8–6.2, temperature of $20 \text{ }^\circ\text{C}$, unregulated ionic strength ($< 10^{-4} \text{ M}$)

a result of AgNP oxidative dissolution was also determined after 15 and 30 days of storage. It was found that the concentration of silver ions increased with time. The content of leached silver ions determined in the effluents was dependent on the type of AgNP suspension (Table S1). It was established that negatively charged TCSB-AgNPs were the least susceptible to oxidative dissolution. The highest silver ion concentration was found in the effluent collected from the CHSB-AgNP suspension after the longest period of time storage (Table S1). It is worth mentioning that these results indicated that each type of AgNP suspension contained silver ions. Nevertheless, in each case, the concentration of silver ions was significantly lower than the concentration of NPs appearing in the nonionic form.

3.2 Test Phytotestkit

Figure 3 shows the germination, root length, and germination index of model plants after 3 days of exposure to AgNPs and silver ions delivered in the form of AgNO_3 . The germination inhibition was up to 20% for common wheat, 14% for garden cress, 7% for sorghum, and 3% for white mustard (Fig. S1). The greatest inhibition of common wheat seed germination was caused by silver ions delivered in the form of AgNO_3 . Each type of AgNPs and silver ions used in the experiment inhibited the growth of common wheat and garden cress roots as compared to the control. The highest inhibition of root growth was observed after the exposure on CHSB-AgNPs – at the level of 24% for common wheat and 30% for garden cress (Fig. S2, Fig. 4). AgNPs and silver ions reduced the germination index of common wheat and

garden cress also. It was observed that silver ions delivered in the form of AgNO_3 was more toxic for the monocots, while positively charged CHSB-AgNPs were more toxic for the dicots.

3.3 Pot Experiment

The effect of AgNPs and silver ions delivered in the form of AgNO_3 on the morphology of shoots of the plants and electrolyte leakage (EL) is shown in Fig. 5. The greatest decrease in parameters was observed after the use of positively charged CHSB-AgNPs, followed by silver ions delivered in the form of AgNO_3 . There were no significant differences between both types of negatively charged AgNPs. No differences were noted between untreated and exposed to TCSB-AgNPs plants, except for garden cress. AgNPs and silver ions delivered in the form of AgNO_3 used inhibited the dry weight of the shoots of white mustard. The applied AgNPs and silver ions did not affect the dry weight of shoots and EL of the sorghum and garden cress. CHSB-AgNPs and silver ions delivered in the form of AgNO_3 caused significantly higher disintegration of cell membranes of common wheat leaf tissues and in the case of white mustard only CHSB-AgNPs.

Spider plots (Fig. 6) showing phenomenological energy fluxes per excited cross section (CS) and per reaction center (RC) for common wheat, sorghum, and white mustard grown without (control) and under silver ions delivered in the form of AgNO_3 and AgNPs treatment revealed some differences. In common wheat, all treatments groups except TCSB-AgNPs decreased light energy absorption flux per

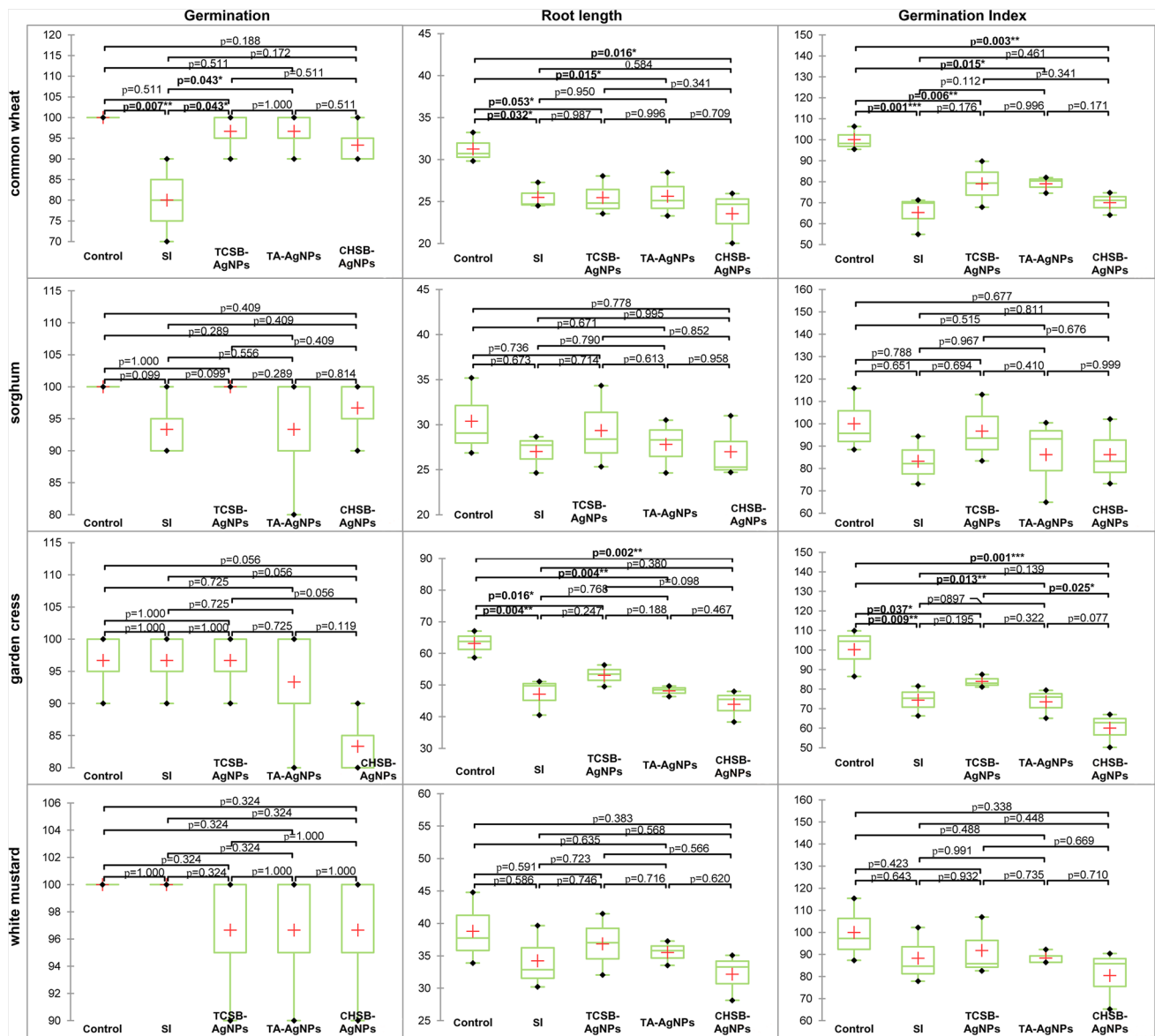


Fig. 3 Boxplots for parameters of Phytotestkit test. The values in the same boxplot set with different superscripts are significantly different from the control group (C) * $p < 0.05$, ** $p < 0.01$, *** $p < 0.001$. Abbreviation: SI, silver ions delivered in the form of AgNO₃

CS (ABS/CS) and trapped energy flux per CS (TR_0/CS), but only CHSB-AgNPs treatment contributed to the decrease in dissipated energy flux per CS (DI_0/CS). In sorghum, CHSB-AgNPs affected all specific energy fluxes parameters and density of reaction centers (RC/CS_0). Energy absorption and energy dissipation were decreased also by silver ions delivered in the form of AgNO₃. Since the density of reaction centers induced by CHSB-AgNPs decreased, sorghum plants compensated by increasing specific energy fluxes per reaction center (RC). However, a significant decrease in OEC was observed. In white mustard, a decrease in electron transport flux (ET_0/CS) and density of reaction centers Rc/CS_0 was also observed under the influence of CHSB-AgNPs and

a decrease in Rc/CS_0 under the influence of silver ions delivered in the form of AgNO₃ compared to controls. Similarly to sorghum, a decrease in the density of reaction centers induced by silver ions delivered in the form of AgNO₃ was accompanied by an increase in TR_0/RC , ET_0/RC , and DI_0/RC . In white mustard, silver ions delivered in the form of AgNO₃ and CHSB-AgNPs contributed also to the decrease in OEC. No changes in ϕE_0 and ψO parameters which mainly reflect the functioning of the PSII electron acceptor side were observed in any of the studied species.

The PCoA results made it possible to ungroup the observations between plants; however, the breakdown of the results by AgNPs was not so clear, especially in garden

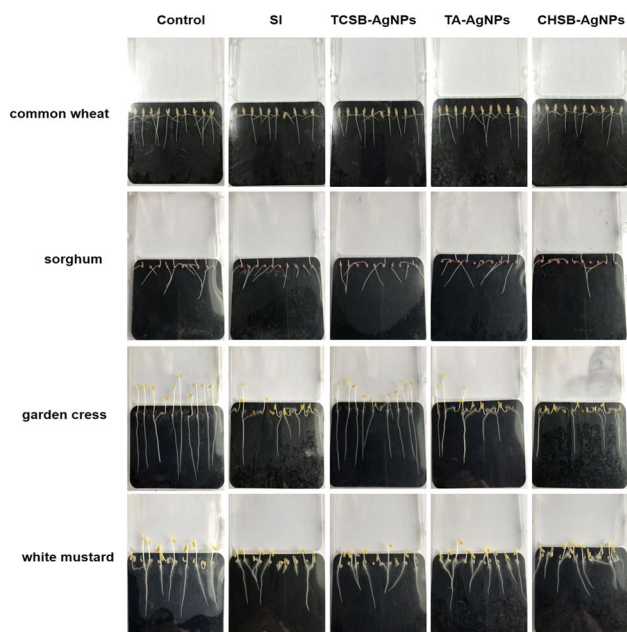


Fig. 4 Photographic representation of roots treated with AgNPs and silver ions delivered in the form of AgNO_3 . Abbreviation: SI, silver ions delivered in the form of AgNO_3

crass (Fig. 7a). Three groups of white mustard, garden cress, and the most diverse sorghum-common wheat were obtained. Based on the results of the agglomeration hierarchical grouping analysis, a clear grouping of plants into two clades consisting of monocotyledons and dicotyledons was observed (Fig. 7b). By analyzing the arrangement of the AHC dendrogram for the distribution of variants, it was observed that two groups were formed in the clade consisting of monocotyledons. The group consisting of 4 variants (from left) showed very low dissimilarity and consisted of TCSB-AgNPs variants and untreated plants. The second group was divided into two subgroups consisting of common wheat and sorghum. Within both subgroups, the impact of the applied measures, i.e., CHSB-AgNPs, silver ions delivered in the form of AgNO_3 and TA-AgNPs, had a similar effect. The second clade consisted of two groups, the first consisting of a little differentiated garden cress and the second – white mustard – consisting of a proportionally increasing dissimilarity: TA-AgNPs, TCSB-AgNPs < silver ions delivered in the form of AgNO_3 < CHSB-AgNPs < control.

The biplots PCA for each plant is shown separately in Fig. 7c. In each cases, the first two factors (F1 and F2) allow us to represent high values of the initial variability of the data, i.e., 87.34% for common wheat, 85.96% for sorghum, 96.32% for garden cress, and 89.72% for white mustard, respectively. The individual PCA biplots indicated a similar interaction of AgNPs regardless of the plant species. The effect of nanoparticles on common wheat showed that TCSB-AgNPs had only a negligible effect on plant

development parameters. Nevertheless, TCSB-AgNPs had a better influence on the development of the phyllosphere and improved photosynthetic parameters such as ψ_0 , TR_0/CS , ET_0/CS , ABS/CS , and RC/CS_0 , while untreated plants showed longer roots, OEC, ϕE_0 , and germination index. On the other hand, CHSB-AgNPs and silver ions delivered in the form of AgNO_3 had the strongest effect on the deterioration of almost all plant development parameters. In both of these variants, clear disintegration of cell walls (EL) and increase of photosynthesis parameters, such as ABS/RC , TR_0/RC , and ET_0/RC , were observed, which was inversely correlated with the length of roots, germination index, OEC, ϕE_0 , and DI_0/CS and the length of shoots ($R > 0.8$). When analyzing the influence of variants on plant development, it was observed that TCSB-AgNPs had no global effect on the plant compared to control. On the other hand, CHSB-AgNPs had the strongest influence on the development parameters of sorghum. The CHSB-AgNPs was the only one to have a strong association with EL and ABS/RC . The electrolyte outflows were inversely correlated with all biometric and part of the photosynthetic parameters, i.e., ET_0/CS , RC/CS_0 , TR_0/CS , DI_0/CS , and ABS/CS , and correlated only with ABS/RC . The influence of silver compounds on biometric parameters of garden cress was the weakest in the case of TCSB-AgNPs, indirect in the case of TA-AgNPs, and the strongest in the case of silver ions delivered in the form of AgNO_3 and CHSB-AgNPs. All biometric parameters, except germination, were strongly correlated with each other, and their high value characteristic for the control variant and, to a lesser extent, TCSB-AgNPs was inversely correlated with EL. In the case of white mustard, it was observed that high EL values are characteristic of the CHSB-AgNPs and silver ions delivered in the form of AgNO_3 variants are inversely correlated with almost all biometric and photosynthetic parameters, while all high values of DI_0/RC , ABS/RC , ET_0/RC , and TR_0/RC parameters are characteristic of the silver ions variant and are inversely correlated especially with ABS/CS , DI_0/CS , OEC, and dry weight of shoots. A smaller similarity of the TCSB-AgNPs variant to the control was also observed in this plant.

4 Discussion

The seed germination was the first parameter used to evaluate the sensitivity of the tested plants to the AgNPs and silver ions delivered in the form of AgNO_3 . In the experiment, only common wheat reacted with a decrease in seed germination after the treatment with silver ions delivered in the form of AgNO_3 , while no significant effect of the AgNPs on the seed germination of plants was observed. Probably it may be related to the structure of seed coats, which show selective permeability to various substances,

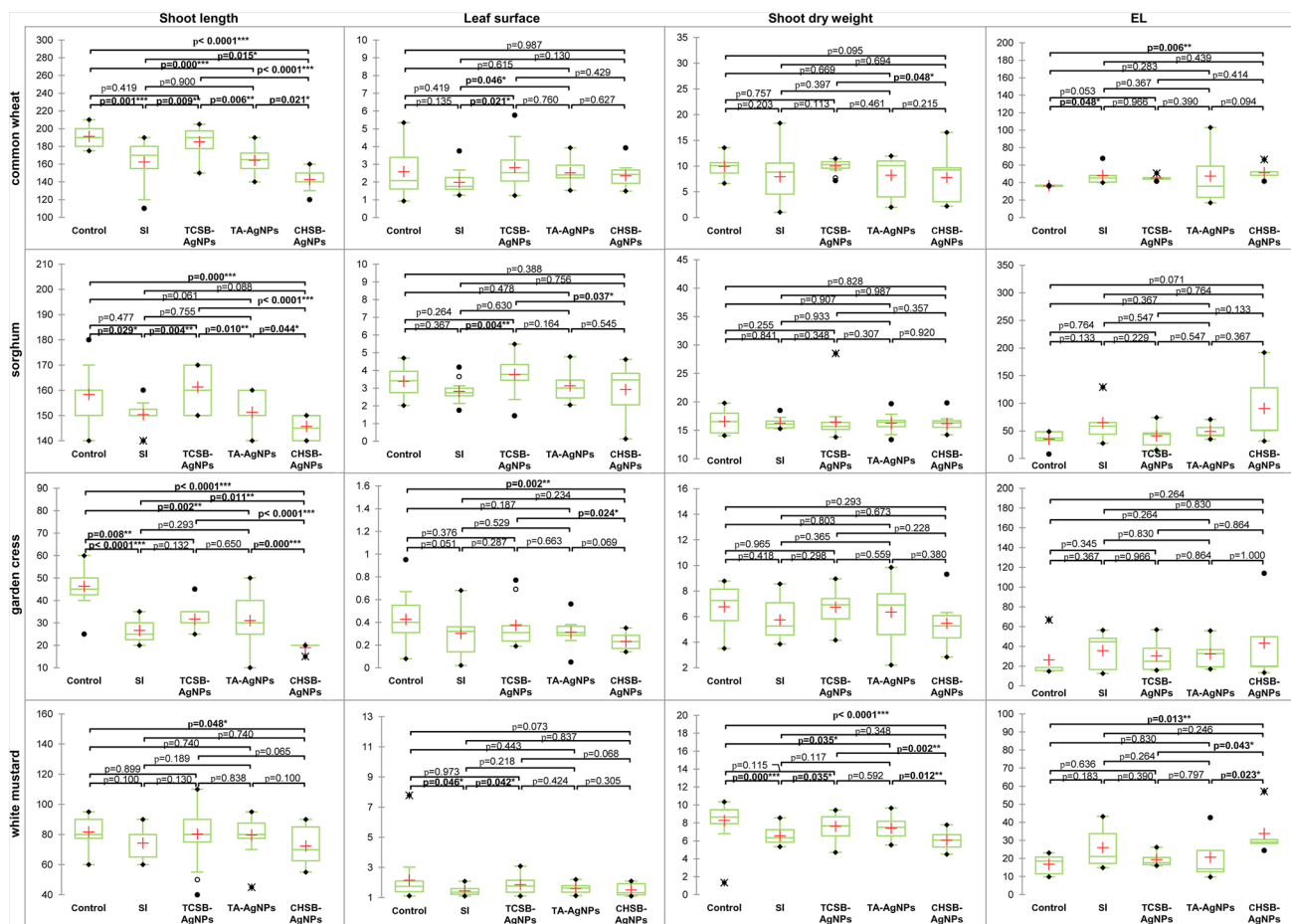


Fig. 5 Boxplots for the shoot morphology of model plants and EL in pot experiment. The values in the same boxplot set with different superscripts are significantly different from the control group

thus protecting the embryo against harmful external factors (Lin and Xing 2007). Our results are confirmed by the studies by Joško and Oleszczuk (2013, 2014), who did not note a significant effect of zinc oxide (ZnO), titanium dioxide (TiO₂), and nickel (Ni) NPs on the germination of garden cress seeds. The primary NPs size, surface area, and zeta potential were as follows: ZnONPs < 100 nm, 15–25 m² g⁻¹, 1.53 mV; TiO₂NPs < 21 nm, 35–65 m² g⁻¹, -7.30 mV; and NiNPs < 100 nm, 8–12 m² g⁻¹, 15.53 mV, respectively. Lin and Xing (2007) also failed to show a significant effect of the selected NPs characterized with different size and primary surface area, respectively: aluminum (AlNPs), 18 nm, 50 m² g⁻¹; alumina (Al₂O₃NPs), 60 nm, 180 m² g⁻¹; zinc (ZnNPs), 35 nm, 40 m² g⁻¹; zinc oxide (ZnONPs), 20 nm, 50 m² g⁻¹; and multi-walled carbon nanotube (MWCNT), 10–20 nm, 400–300 m² g⁻¹, on radish, rape, ryegrass, lettuce, corn, and cucumber sprouting. The exception was ZnNPs, which inhibited ryegrass sprouting, and in the case of maize – ZnONPs. In turn, AgNPs synthesized by reduction of AgNO₃ with trisodium citrate (Na₃C₆H₅O₇·2H₂O)

(C) **p* < 0.05, ***p* < 0.01, ****p* < 0.001. Abbreviation: SI, silver ions delivered in the form of AgNO₃

and size in the range of 10 to 20 nm (Razzaq et al. 2016) and AgNPs synthesized under the action of “green” reagent glucose and average size of about 10 nm (Asanova et al. 2019) in low concentrations did not affect the germination of wheat seeds, while after exceeding a certain concentration, they limited this parameter. According to Cruz et al. (2013), the interspecific differences observed in terms of seed germination result from different seed sizes. Larger seeds are characterized by a smaller surface area in relation to the volume, which provides greater protection against various contaminants. This relationship was not confirmed in our study, because the size of the seed material used was in the following order sorghum > common wheat > white mustard > garden cress and the sensitivity to the tested compounds did not differ significantly between the plants.

Many plants exposed to metal stress germinate in a polluted environment but then stop growing. Roots are the first organ to be exposed to toxic factors found in substrates and therefore react to these stress conditions mainly by inhibiting growth. This thesis was confirmed by the results of our

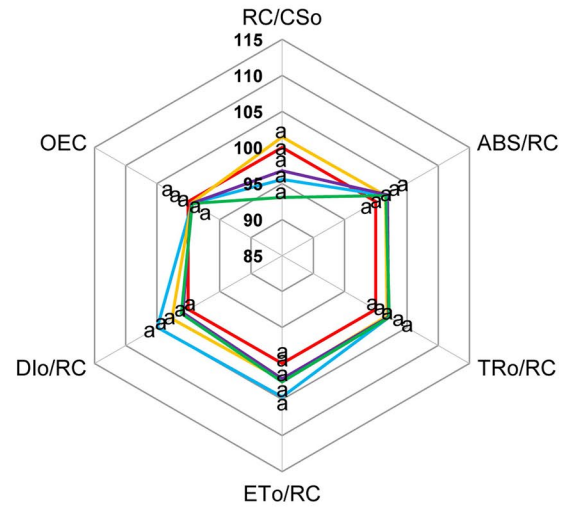
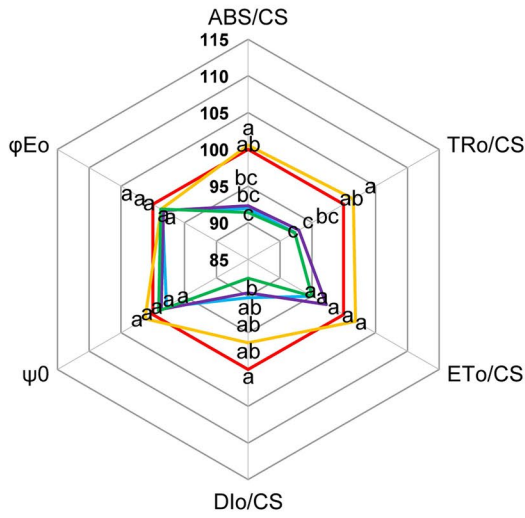
studies, which showed a significant inhibition of common wheat and garden cress roots exposed to the AgNPs and silver ions delivered in the form of AgNO_3 . CHSB-AgNPs were the most toxic for the plants which may be related to the surface properties of the NPs resulting from the preparation method. Milewska-Hendel et al. (2019) also showed high toxicity of positively charged gold nanoparticles (AuNPs+) to roots of barley cv. Karat. The average root length of the control plants was 3.9 mm, while the plants treated with AuNPs (+) in the concentration of 25 mg L^{-1} –3.6 mm and AuNPs (+) in the concentration of 50 mg L^{-1} –2.9 mm. In addition, the authors found that AuNPs (+) disrupted cellular symplasmic communication, which led to a hairless root phenotype, thus limiting the proper functioning of the roots. It has been proven that the NPs surface properties, including the surface charge of NPs, can influence their reactivity, penetration, and translocations in plants (Rastogi et al. 2017). Spielman-Sun et al. (2017) showed that positively charged cerium oxide nanoparticles CeO_2NPs (+) bind to wheat roots more than negatively charged ones (CeO_2NPs (-)). The effect was explained in terms of the electrostatic interaction between CeO_2NPs (+) and the negatively charged root surface. Plants treated for 34 h with CeO_2NPs (+) had a lower concentration of Ce in the leaves than plants treated with CeO_2NPs (-) and neutral CeO_2NPs (0), which means that they are less transferred from the roots to the shoots. These results are confirmed by the research conducted by Spielman-Sun et al. (2019) for monocotyledons (corn and rice) and dicotyledons (tomato and lettuce) treated with CeO_2NPs and Zhu et al. (2012) in the case of rice, radish, pumpkin, and perennial ryegrass exposed to AuNPs.

In the study, the applied AgNPs and silver ions delivered in the form of AgNO_3 reduced not only the length of the roots but also significantly limited the length of the shoots of common wheat, sorghum, and garden cress; surface of the leaves of garden cress and white mustard; and the dry mass of white mustard shoots. The positively charged CHSB-AgNPs and silver ions delivered in the form of AgNO_3 showed the greatest inhibition effect. These results suggest that the surface properties of AgNPs play a significant role in the mechanisms of their biological activity. On the other hand, one can also indicate that observed effects can be related to the differences in structure between plants monocotyledonous and dicotyledonous. Our results confirmed previous reports on the harmful effects of AgNPs and other silver compounds on the above-ground parts of higher plants (Dimkpa et al. 2013; Vannini et al. 2014; Wang et al. 2020; Yang et al. 2018; Zuverza-Mena et al. 2016). Jhanzab et al. (2015) noted that AgNPs synthesized chemically by the reduction of AgNO_3 with trisodium citrate dehydrate in high concentrations limited the leaf surface of wheat, while lower concentrations had a positive effect on this parameter. This effect is called hormesis, i.e., a two-phase dose response in

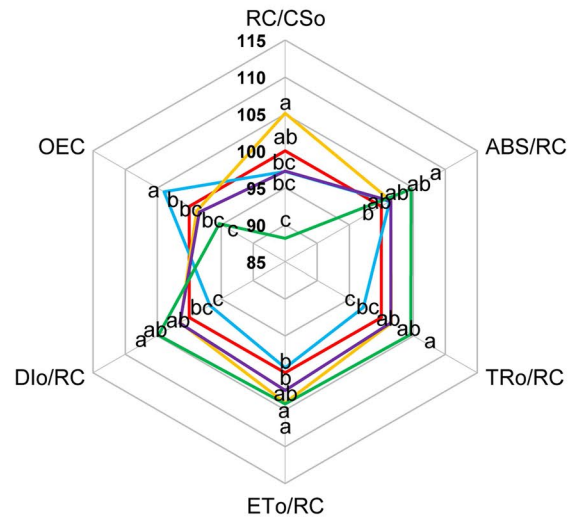
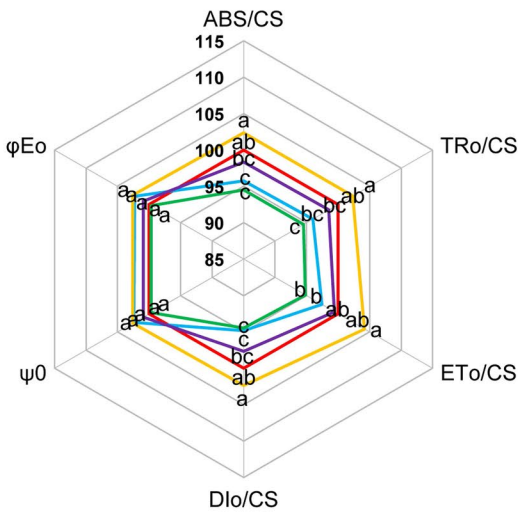
which the presence of small doses has a beneficial effect on the organism while being harmful in the range of higher doses (Agathokleous et al. 2019; Calabrese 2014; Poschenrieder et al. 2013). These results are in line with the results obtained by Salama (2012) for common bean and maize and Razzaq et al. (2016) in the case of wheat. In the work of the last author, it was found that not only the concentration but also the duration of exposure could affect the hormetic response of wheat. Therefore, it can be concluded that the activity of NPs depends not only on their surface properties but is also largely determined by the concentration used and the exposure time.

Light reaction in plants starts with the absorption of light energy by antennae. The efficiency of this process reflects absorption flux per CS (ABS/CS). In turn specific energy fluxes (ET_0 , TR_0 , DI_0) per CS quantify the photosystem II behavior. Our results show that no significant difference in the ABS/CS, between the control and treatment groups, was only in white mustard indicating that in this species the all treatments did not affect energy absorption but affect energy flow from PSII. In white mustard, the changes induced were mainly due to CHSB-AgNPs and silver ions delivered in the form of AgNO_3 , which decreased energy fluxes per CS and the amount of active PSII RCs per CS, but solely after silver ions treatment were they compensated by an increase in electron transport flux and energy trapped flux per RC. The absorption efficiency of light energy was affected by silver ions delivered in the form of AgNO_3 and mainly CHSB-AgNPs treatment in wheat and sorghum plants. However, treatment of sorghum plants only with CHSB-AgNPs resulted in increased energy fluxes per reaction center. As shown in the spider plots, majority of presented parameters in all tested species were affected to a different extent by positively charged CHSB-AgNPs and silver ions delivered in the form of AgNO_3 treatment but were not significantly changed by negatively charged TCSB-AgNPs. Hence, CHSB-AgNPs could reduce the energy conversion efficiency of PSII, in greater extent than TA-AgNPs (negatively charged) which affected ABS/CS and TR_0/CS but only in wheat. In general, PSII of investigated model plants was thus more sensitive to silver ions delivered in the form of AgNO_3 and positively charged CHSB-AgNPs, thus indicating significant role of surface properties of AgNPs. Changes in light reaction seems to be important for assessment of influence AgNPs on plants photosynthetic apparatus since a dominant role in the decreasing photosynthesis plays non-stomatal limitation as demonstrated by Liu et al. (2020) in response to $\text{La}_2\text{O}_3\text{NPs}$. In the current work, the light reaction of wheat (monocot) and white mustard (dicot) C3 pathway species is compared to sorghum, which utilize the C4 photosynthetic mechanism. According some studies NPs uptake and toxicity in plants are photosynthetic pathways, C3 and C4 dependent (Bai et al. 2021; Liu et al. 2020). It seems that

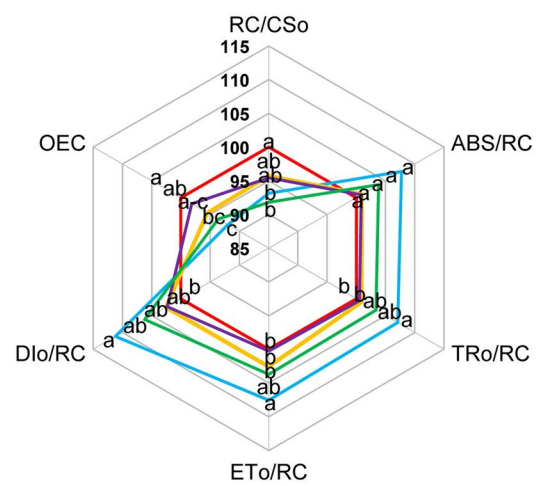
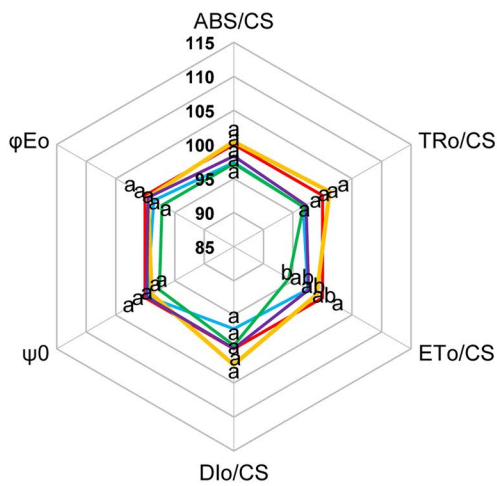
common wheat



sorghum



white mustard



— Control — SI — TCSB-AgNPs — TA-AgNPs — CHSB-AgNPs

Fig. 6 The effect of AgNPs and SI on the efficiency of photosystem II of common wheat, sorghum and white mustard. Values marked with the same letters separately for each tested parameters are not significantly different ($p \leq 0.05$) according to the multiple Duncan's test. Abbreviation: SI, silver ions delivered in the form of AgNO_3

wheat monocot C3 plant is less sensitive to AgNPs because wheat not declined the amount of active PSII RCs per CS. Although studies by other authors show that NPs uptake in the C3 species wheat and rice was greater than that in C4 plants amaranth and maize (Bai et al. 2021). For example, the La_2O_3 NPs restricted carbon fixation in C4 maize, while in C3 soybean, they inhibited the electron transport (Liu et al. 2020). C4 plants are generally more tolerant to heavy metals than C3 plants, which is usually due to higher water use efficiency in C4 plants (Bai et al. 2021). Additionally monocots are less likely to take up nanoparticles because water uptake in monocot wheat is lower to that of dicot pumpkin (Siddiqi and Husen 2017). In contrast in the current study, sorghum seems to be the most sensitive to the AgNPs, particularly positively charged CHSB-AgNPs.

Plant exposure to metal stress often negatively affects the integrity and permeability of the cell membrane (Ma et al. 2015; Yan and Chen 2019). The indicator of the degree of damage to cell membranes is the measurement of the outflow of electrolytes (ions, amino acids, organic acids, etc.) flowing out of the examined tissue (Demidchik et al. 2014). In our experiment, while assessing the outflow of electrolytes from the leaves of the tested plants, it was noticed that each type of AgNPs and silver ions delivered in the form of AgNO_3 caused a significantly higher disintegration of cell membranes in common wheat and white mustard leaf tissues compared to the control. CHSB-AgNPs turned out to be the most toxic. This may be due to their surface properties and size. Among all tested AgNPs, CHSB-AgNPs were characterized by the smallest size (Table S1). Smaller particles have a larger active surface area. In addition, they can more easily penetrate plant cell membranes and interfere with the metabolic activity of the cell. On the other hand, under the adopted experimental conditions, no significant effect of the AgNPs and silver ions delivered in the form of AgNO_3 was found on the level of damage to the cell membranes of sorghum and garden cress leaf tissues, although the observed tendency indicated that all silver compounds increased this parameter in comparison with the control. Gorczyca et al. (2015) noted that the leakage of electrolytes measured in the leaves of common wheat showed no significant differences between the applied treatments, while in the roots, it doubled under the influence of AgNPs produced using the high-voltage arc discharge method compared to the control group. Increased electrolyte leakage is a result of a reactive oxygen species (ROS) impairment of membrane integrity (Anjum et al. 2013). Barbasz et al. (2018) showed that negatively

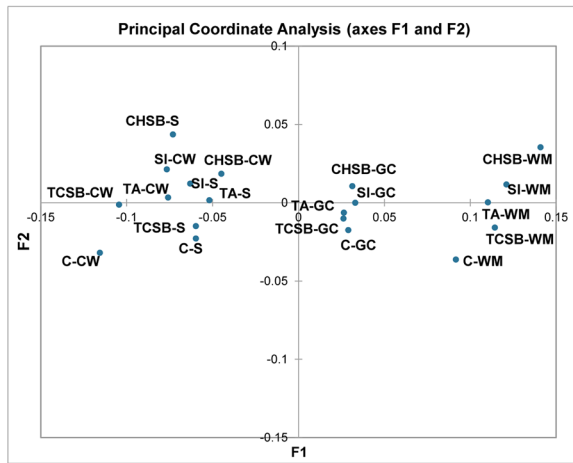
charged AgNPs obtained with the use of sodium borohydride (SBNM-AgNPs) and trisodium citrate (SBTC-AgNPs) as well as positively charged cysteamine-stabilized AgNPs (SBATE-AgNPs) were toxic to callus cells of two spring wheat cultivars. The highest toxicity is reported in the case of SBATE-AgNPs. The tested compounds increased the concentration of proline and peroxidation of membrane lipids, as well as increased superoxide dismutase activity (SOD), which proves the presence of oxidative stress in cells. Other researchers also reported increased ROS production in plant cells after treatment with AgNPs and SI (Barbasz et al. 2016; Cvjetko et al. 2017; Hossain et al. 2015; Nair and Chung 2014; Tripathi et al. 2017; Yan and Chen 2019). Oxidative stress can initiate a defense mechanism in plant cells by increasing the activity of antioxidant enzymes (Karimi and Mohsenzadeh 2017; Rastogi et al. 2019).

Based on the results of AHC and PCoA, it was observed that in terms of the global impact of AgNPs, their impact is different in the case of monocotyledonous and dicotyledonous plants, but the size of the changes is not significant, so it concerns individual parameters. Only individual PCAs revealed the strength of the interaction, which was generally similar in all the tested plants, i.e., control < TCSB-AgNPs < TA-AgNPs < silver ions delivered in the form of AgNO_3 < CHSB-AgNPs, where TCSB-AgNPs had the weakest effect on the analyzed parameters, and CHSB-AgNPs had the strongest effect, with a clear outflow of electrolytes from the shoot tissues.

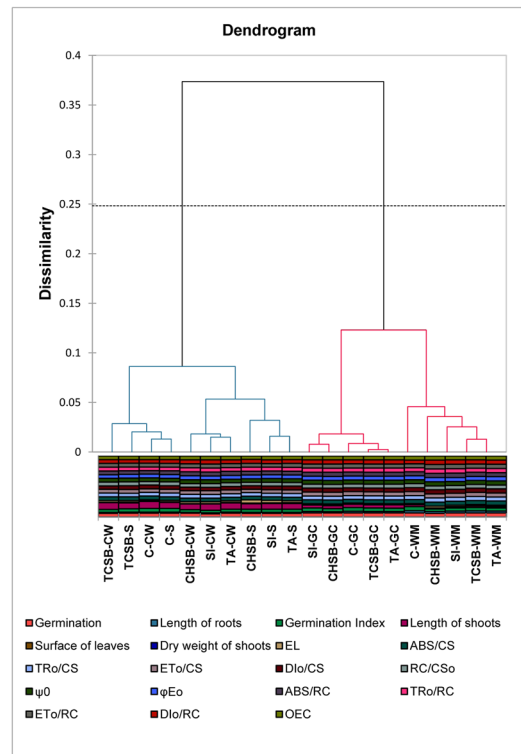
5 Conclusions

The obtained results indicate that the response of monocot and dicot plants to AgNPs and silver ions delivered in the form of AgNO_3 was different. All silver compounds at a concentration of 50 mg L^{-1} had a similar effect regardless of the plant species. Negatively charged AgNPs (TCSB-AgNPs) had the weakest effect on the analyzed parameters, while positively charged AgNPs (CHSB-AgNPs) had the strongest effect. The results showed that the surface charge of AgNPs and their surface properties resulting from the reduction method during the preparation of silver suspensions are relevant for the initial development of the model plants. CHSB-AgNPs and silver ions delivered in the form of AgNO_3 adversely affected almost all development parameters of model plants. In both of these treatments, clear electrolyte outflows, which reflect damage to the cell membrane of plant leaf tissues and elevated values of photosynthesis parameters defining phenomenological energy fluxes per reaction center (RC), were observed. The exception is sorghum, in the case of which silver ions delivered in the form

a)



b)



c)

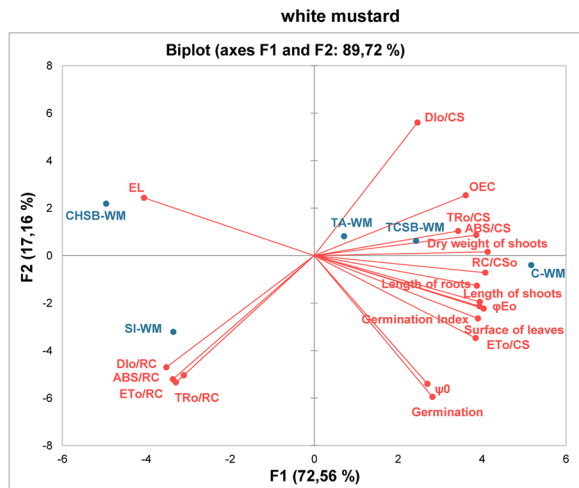
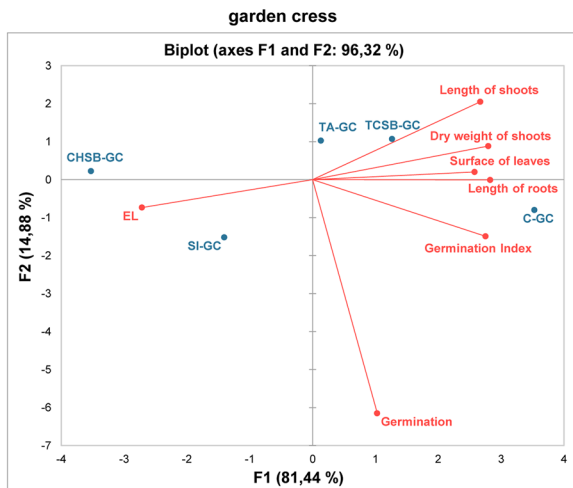
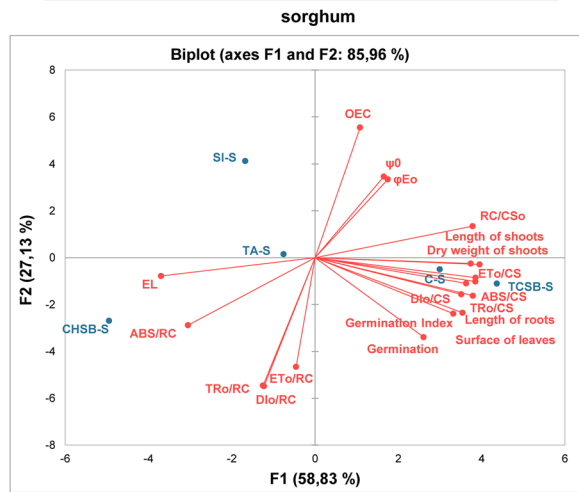
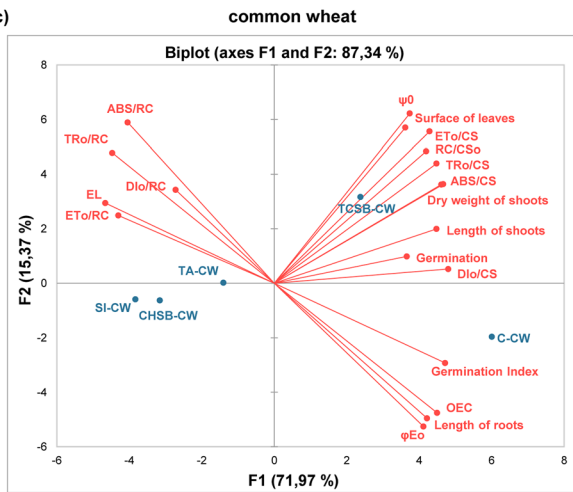


Fig. 7 Interaction between silver compounds and plants on basis of principal coordinates analysis (a), agglomerative hierarchical clustering (b), and principal component analysis (c). Abbreviations: CW, common wheat; S, sorghum; GC, garden cress; WM, white mustard; SI, silver ions delivered in the form of AgNO_3

of AgNO_3 did not have a negative impact on these parameters, but also did not have a positive effect on the other developmental traits.

Supplementary Information The online version contains supplementary material available at <https://doi.org/10.1007/s42729-022-00760-9>.

Acknowledgements The authors would like to thank Professor Stanisław Walas from the Jagiellonian University for the AAS measurements. The authors are also grateful to Doctor Dorota Duraczyńska for the imaging of AgNPs using electron microscopy.

Author Contribution Conceptualization: EM, AG; Data curation: EM, MO; Formal analysis: EM; Funding acquisition: EM, EP, MO; Investigation: EM, MO; Methodology: AG, EP, MO; Project administration: EM; Software: EM, SWP; Validation: EM, EP, SWP, MO; Visualization: EM, SWP; Writing—original draft: EM, EP, SWP, MO; Writing—review and editing: EM.

Funding This work is supported by subsidy of the Ministry of Science and Higher Education for UR Krakow in a year 2020 number 010012-D011 and 010014-D11. This research partially founded by the statutory research found of ICSC PAS.

Declarations

Conflict of Interest The authors declare no competing interests.

Open Access This article is licensed under a Creative Commons Attribution 4.0 International License, which permits use, sharing, adaptation, distribution and reproduction in any medium or format, as long as you give appropriate credit to the original author(s) and the source, provide a link to the Creative Commons licence, and indicate if changes were made. The images or other third party material in this article are included in the article's Creative Commons licence, unless indicated otherwise in a credit line to the material. If material is not included in the article's Creative Commons licence and your intended use is not permitted by statutory regulation or exceeds the permitted use, you will need to obtain permission directly from the copyright holder. To view a copy of this licence, visit <http://creativecommons.org/licenses/by/4.0/>.

References

- Agathokleous E, Kitao M, Calabrese EJ (2019) Hormesis: a compelling platform for sophisticated plant science. *Trends Plant Sci* 24:318–327. <https://doi.org/10.1016/j.tplants.2019.01.004>
- Akter M, Sikder MT, Rahman MM, Ullah AKMA, Hossain KFB, Banik S, Hosokawa T, Saito T, Kurasaki M (2017) A systematic review on silver nanoparticles-induced cytotoxicity: physicochemical properties and perspectives. *J Adv Res* 9:1–16. <https://doi.org/10.1016/j.jare.2017.10.008>
- Angiosperm Phylogeny Group, Chase MW, Christenhusz MJM, Fay MF, Byng JW, Judd WS, Soltis DE, Mabberley DJ, Sennikov AN, Soltis PS, Stevens PF (2016) An update of the Angiosperm Phylogeny Group classification for the orders and families of flowering plants: APG IV. *Bot J Linn Soc* 181:1–20. <https://doi.org/10.1111/boj.12385>
- Anjum NA, Gill SS, Duarte AC, Pereira E, Ahmad I (2013) Silver nanoparticles in soil–plant systems. *J Nanopart Res* 15:1896. <https://doi.org/10.1007/s11051-013-1896-7>
- Asanova AA, Yashin SE, Trofimova TV, Polonskiy VI (2019) Application of silver nanoparticles to improve wheat seedlings growth. *IOP Con Ser Earth Environ Sci* 315:052041. <https://doi.org/10.1088/1755-1315/315/5/052041>
- Bai T, Zhang P, Guo Z, Chetwynd AJ, Zhang M, Adeel M, Li M, Guo K, Gao R, Li J, Hao Y, Rui Y (2021) Different physiological responses of C3 and C4 plants to nanomaterials. *Environ Sci Pollut Res* 28:25542–25551. <https://doi.org/10.1007/s11356-021-12507-7>
- Barbasz A, Kreczmer B, Oćwieja M (2016) Effects of exposure of callus cells of two wheat varieties to silver nanoparticles and silver salt (AgNO_3). *Acta Physiol Plant* 38:76. <https://doi.org/10.1007/s11738-016-2092-z>
- Barbasz A, Oćwieja M, Roman M (2017) Toxicity of silver nanoparticles towards tumoral human cell lines U-937 and HL-60. *Colloids Surf B* 156:397–404. <https://doi.org/10.1016/j.colsurfb.2017.05.027>
- Barbasz A, Kreczmer B, Oćwieja M (2018) How the surface properties affect the nanocytotoxicity of silver? Study of the influence of three types of nanosilver on two wheat varieties. *Acta Physiol Plant* 40:1–7. <https://doi.org/10.1007/s11738-018-2613-z>
- Calabrese EJ (2014) Hormesis: a fundamental concept in biology. *Microb Cell* 1:145–149. <https://doi.org/10.15698/mic2014.05.145>
- Chen Y, Xie Y, Song C, Zheng L, Rong X, Jia L, Luo L, Zhang C, Qu X, Xuan W (2018) A comparison of lateral root patterning among dicot and monocot plants. *Plant Sci* 274:201–211. <https://doi.org/10.1016/j.plantsci.2018.05.018>
- Chichiricò G, Poma A (2015) Penetration and toxicity of nanomaterials in higher plants. *Nanomaterials (Basel)* 5:851–873. <https://doi.org/10.3390/nano5020851>
- Conklin PA, Strable J, Li S, Scanlon MJ (2019) On the mechanisms of development in monocot and eudicot leaves. *New Phytol* 221:706–724. <https://doi.org/10.1111/nph.15371>
- Cox A, Venkatachalam P, Sahi S, Sharma N (2017) Reprint of: silver and titanium dioxide nanoparticle toxicity in plants: a review of current research. *Plant Physiol Biochem* 110:33–49. <https://doi.org/10.1016/j.plaphy.2016.08.007>
- Cruz JM, Lopes PRM, Montagnolli RN, Tamada IS, Silva NMMG, Bidoia ED (2013) Toxicity assessment of contaminated soil using seeds as bioindicators. *J Appl Biotechnol* 1:1–10. <https://doi.org/10.5296/jab.v1i1.3408>
- Cvjetko P, Milošić A, Domijan AM, Vrček IV, Tolić S, Štefanić PP, Letofsky-Papst I, Tkalec M, Balen B (2017) Toxicity of silver ions and differently coated silver nanoparticles in *Allium cepa* roots. *Ecotoxicol Environ Saf* 137:18–28. <https://doi.org/10.1016/j.ecoenv.2016.11.009>
- Cvjetko P, Zovko M, Štefanić PP, Biba R, Tkalec M, Domijan AM, Vinković Vrček I, Letofsky-Papst I, Šikić S, Balen B (2018) Phytotoxic effects of silver nanoparticles in tobacco plants. *Environ Sci Pollut Res* 25:5590–5602. <https://doi.org/10.1007/s11356-017-0928-8>
- Demidchik V, Straltsova D, Medvedev SS, Pozhvanov GA, Sokolik A, Yurin V (2014) Stress-induced electrolyte leakage: the role of K^+ -permeable channels and involvement in programmed cell death and metabolic adjustment. *J Exp Bot* 65:1259–1270. <https://doi.org/10.1093/jxb/eru004>
- Dimkpa CO, McLean JE, Martineau N, Britt DW, Haverkamp R, Anderson AJ (2013) Silver nanoparticles disrupt wheat (*Triticum aestivum* L.) growth in a sand matrix. *Environ Sci Technol* 47:1082–1090. <https://doi.org/10.1021/es302973y>

- Du J, Tang J, Xu S, Ge J, Dong Y, Li H, Jin M (2018) A review on silver nanoparticles-induced ecotoxicity and the underlying toxicity mechanisms. *Regul Toxicol Pharmacol* 98:231–239. <https://doi.org/10.1016/j.yrtph.2018.08.003>
- Eich J, Dürholt H, Steger-Hartmann T, Wagner E (2000) Specific detection of membrane-toxic substances with a conductivity assay. *Ecotoxicol Environ Saf* 45:228–235. <https://doi.org/10.1006/eesa.1999.1854>
- European Commission (2019) CORDIS results pack on nano-enhanced industrial materials. ISSN 2599–8293
- Evans JR (2013) Improving photosynthesis. *Plant Physiol* 162:1780–1793. <https://doi.org/10.1104/pp.113.2.19006>
- Geisler-Lee J, Wang Q, Yao Y, Zhang W, Geisler M, Li K, Huang Y, Chen Y, Kolmakov A, Ma X (2013) Phytotoxicity, accumulation and transport of silver nanoparticles by *Arabidopsis thaliana*. *Nanotoxicology* 7:323–337. <https://doi.org/10.3109/17435390.2012.658094>
- Gorczyca A, Pocięcha E, Kasprówicz M, Niemiec M (2015) Effect of nanosilver in wheat seedlings and *Fusarium culmorum* culture systems. *Eur J Plant Pathol* 142:251–261. <https://doi.org/10.1007/s10658-015-0608-9>
- Gorczyca A, Pocięcha E, Matras E (2021) Nanotechnology in agriculture, the food sector, and remediation: prospects, relations, and constraints. In: Prasad R (ed) *Environmental pollution and remediation. Environmental and microbial biotechnology*. Springer, Singapore, pp 1–34. https://doi.org/10.1007/978-981-15-5499-5_1
- Gorczyca A, Pocięcha E, Maciejewska-Prończuk J, Kula-Maximenko M, Oćwieja M (2022) Phytotoxicity of silver nanoparticles and silver ions toward common wheat. *Surf Innov* 10:48–58. <https://doi.org/10.1680/jsuin.20.00094>
- Han SK, Torii KU (2016) Lineage-specific stem cells, signals and asymmetries during stomatal development. *Development* 143:1259–1270. <https://doi.org/10.1242/dev.127712>
- Hepworth C, Caine RS, Harrison EL, Sloan J, Gray JE (2018) Stomatal development: focusing on the grasses. *Curr Opin Plant Biol* 41:1–7. <https://doi.org/10.1016/j.pbi.2017.07.009>
- Heyneke E, Fernie AR (2018) Metabolic regulation of photosynthesis. *Biochem Soc Trans* 46:321–328. <https://doi.org/10.1042/BST20170296>
- Hossain Z, Mustafa G, Komatsu S (2015) Plant responses to nanoparticle stress. *Int J Mol Sci* 16:26644–26653. <https://doi.org/10.3390/ijms161125980>
- Hu J, Xianyu Y (2021) When nano meets plants: a review on the interplay between nanoparticles and plants. *Nano Today* 38:101143. <https://doi.org/10.1016/j.nantod.2021.101143>
- Jhazab HM, Razaq A, Jilani G, Rehman A, Hafeez A, Yasmeen F (2015) Silver nanoparticles enhance the growth, yield and nutrient use efficiency of wheat. *Int J Agron Agric Res* 7:15–22. ISSN: 2223-7054 (Print) 2225-3610 (Online)
- Jiang J, Oberdörster G, Biswas P (2009) Characterization of size, surface charge, and agglomeration state of nanoparticle dispersions for toxicological studies. *J Nanopart Res* 11:77–89. <https://doi.org/10.1007/s11051-008-9446-4>
- Joško I, Oleszczuk P (2013) Influence of soil type and environmental condition on ZnO, TiO₂ and Ni nanoparticles phytotoxicity. *Chemosphere* 92:91–99. <https://doi.org/10.1016/j.chemosphere.2013.02.048>
- Joško I, Oleszczuk P (2014) Phytotoxicity of nanoparticles — problems with bioassay choosing and sample preparation. *Environ Sci Pollut Res* 21:10215–10224. <https://doi.org/10.1007/s11356-014-2865-0>
- Kajala K, Covshoff S, Karki S, Woodfield H, Tolley BJ, Dionora MJ, Mogul RT, Mabilangan AE, Danila FR, Hibberd JM, Quick WP (2011) Strategies for engineering a two-celled C(4) photosynthetic pathway into rice. *J Exp Bot* 62:3001–3010. <https://doi.org/10.1093/jxb/err022>
- Karimi J, Mohsenzadeh S (2017) Physiological effects of silver nanoparticles and silver nitrate toxicity in *Triticum aestivum*. *Iran J Sci Technol Trans Sci* 41:111–120. <https://doi.org/10.1007/s40995-017-0200-6>
- Khan I, Saeed K, Khan I (2019) Nanoparticles: properties, applications and toxicities. *Arab J Chem* 12:908–931. <https://doi.org/10.1016/j.arabj.2017.05.011>
- Koushik B, Pragati P, Aniruddha M, Joshi DC, Wani SH, Krishnan P (2019) Methods of using nanomaterials to plant systems and their delivery to plants (mode of entry, uptake, translocation, accumulation, biotransformation and barriers). In: Ghorbanpour M, Wani SH (eds) *Advances in phytonanotechnology: from synthesis to application*. Academic Press, San Diego, pp 123–152. <https://doi.org/10.1016/B978-0-12-815322-2.00005-5>
- Kujda M, Oćwieja M, Adamczyk Z, Bocheńska O, Braś G, Kozik A, Bielańska E, Barbasz J (2015) Charge stabilized silver nanoparticles applied as antibacterial agents. *J Nanosci Nanotechnol* 15:3574–3583. <https://doi.org/10.1166/jnn.2015.9727>
- Lee PC, Meisel DP (1982) Adsorption and surface-enhanced Raman of dyes on silver and gold sols. *J Phys Chem* 86:3391–3395. <https://doi.org/10.1021/j100214a025>
- Lin D, Xing B (2007) Phytotoxicity of nanoparticles: inhibition of seed germination and root growth. *Environ Pollut* 150:243–250. <https://doi.org/10.1016/j.envpol.2007.01.016>
- Linh NM, Verna C, Scarpella E (2018) Coordination of cell polarity and the patterning of leaf vein networks. *Curr Opin Plant Biol* 41:116–124. <https://doi.org/10.1016/j.pbi.2017.09.009>
- Liu Y, Yue L, Wang C, Zhu X, Wang Z, Xing B (2020) Photosynthetic response mechanisms in typical C3 and C4 plants upon La₂O₃ nanoparticle exposure. *Environ Sci Nano* 7:81–92. <https://doi.org/10.1039/c9en00992b>
- Ma C, White JC, Dhankher OP, Xing B (2015) Metal-based nanotoxicity and detoxification pathways in higher plants. *Environ Sci Technol* 49:7109–7122. <https://doi.org/10.1021/acs.est.5b00685>
- Malandrakis AA, Kavroulakis N, Avramidou M, Papadopoulou KK, Tsaniklidis G, Chrysikopoulos CV (2021) Metal nanoparticles: phytotoxicity on tomato and effect on symbiosis with the *Fusarium solani* FsK strain. *Sci Total Environ* 787:147606. <https://doi.org/10.1016/j.scitotenv.2021.147606>
- Milewska-Hendel A, Witek W, Rypień A, Zubko M, Baranski R, Stróż D, Kurczyńska EU (2019) The development of a hairless phenotype in barley roots treated with gold nanoparticles is accompanied by changes in the symplasmic communication. *Sci Rep* 9:4724. <https://doi.org/10.1038/s41598-019-41164-7>
- Naidu KB, Govender P, Adam JK (2015) Biomedical applications and toxicity of nanosilver: a review. *Med Technol SA* 29:13–9. <https://hdl.handle.net/10520/EJC187494>
- Nair PM, Chung IM (2014) Physiological and molecular level effects of silver nanoparticles exposure in rice (*Oryza sativa* L.). *Chemosphere* 112:105–113. <https://doi.org/10.1016/j.chemosphere.2014.03.056>
- Navarro E, Baun A, Behra R, Hartmann NB, Filser J, Miao AJ, Quigg A, Santschi PH, Sigg L (2008) Environmental behavior and ecotoxicity of engineered nanoparticles to algae, plants, and fungi. *Ecotoxicology* 17:372–386. <https://doi.org/10.1007/s10646-008-0214-0>
- Nayyar H, Gupta D (2006) Differential sensitivity of C-3 and C-4 plants to water deficit stress: association with oxidative stress and antioxidants. *Environ Exp Bot* 58:106–113. <https://doi.org/10.1016/j.envexpbot.2005.06.021>
- Oćwieja M, Adamczyk Z, Morga M, Michna A (2011) High density silver nanoparticle monolayers produced by colloid self-assembly on polyelectrolyte supporting layers. *J Colloid Interface Sci* 364:39–48. <https://doi.org/10.1016/j.jcis.2011.07.059>
- Oćwieja M, Gorczyca A, Niemiec M, Pocięcha E, Adamczyk Z (2014) Effect of charge-stabilized silver nanoparticles with various surface

- properties on physiological stage of seedlings of *Triticum aestivum*. FEBS J 281:622–623
- Oćwieja M, Barbasz A, Walas S, Paluszkiwicz C (2017) Physicochemical properties and cytotoxicity of cysteine-functionalized silver nanoparticles. Colloids Surf B Biointerfaces 160:429–437. <https://doi.org/10.1016/j.colsurfb.2017.09.042>
- Parry MA, Andralojc PJ, Scales JC, Salvucci ME, Carmo-Silva AE, Alonso H, Whitney SM (2013) Rubisco activity and regulation as targets for crop improvement. J Exp Bot 64:717–730. <https://doi.org/10.1093/jxb/ers336>
- Phytotoxkit (2004) Seed germination and early growth microbistest with higher plants. Standard Operation Procedure. MicroBioTests Inc., Nazareth, pp 1–24
- Pinsino A, Bastús NG, Busquets-Fité M, Canesi L, Cesaroni P, Drobne D, Duschl A, Ewart MA, Gispert I, Horejs-Hoeck J, Italiani P, Kemmerling B, Kille P, Procházková P, Puentes VF, Spurgeon DJ, Svendsen C, Wilde CJ, Boraschi D (2020) Probing the immune responses to nanoparticles across environmental species. A perspective of the EU Horizon 2020 project PANDORA. Environ Sci Nano 7:3216–3232. <https://doi.org/10.1039/D0EN00732C>
- Poschenrieder C, Cabot C, Martos S, Gallego B, Barceló J (2013) Do toxic ions induce hormesis in plants? Plant Sci 212:15–25. <https://doi.org/10.1016/j.plantsci.2013.07.012>
- Pradas Del Real AE, Vidal V, Carrière M, Castillo-Michel H, Levard C, Chaurand P, Sarret G (2017) Silver nanoparticles and wheat roots: a complex interplay. Environ Sci Technol 51:5774–5782. <https://doi.org/10.1021/acs.est.7b00422>
- Rajput V, Minkina T, Mazarji M, Shende S, Sushkova S, Mandzhieva S, Burachevskaya M, Chaplygin V, Singh A, Jatav H (2020) Accumulation of nanoparticles in the soil-plant systems and their effects on human health. Ann Agric Sci 65:137–143. <https://doi.org/10.1016/j.aos.2020.08.001>
- Rastogi A, Zivcak M, Sytar O, Kalaji HM, He X, Mbarki S, Brestic M (2017) Impact of metal and metal oxide nanoparticles on plant: a critical review. Front Chem 5:78. <https://doi.org/10.3389/fchem.2017.00078>
- Rastogi A, Zivcak M, Tripathi DK, Yadav S, Kalaji HM, Brestic M (2019) Phytotoxic effect of silver nanoparticles in *Triticum aestivum*: improper regulation of photosystem I activity as the reason for oxidative damage in the chloroplast. Photosynthetica 57:209–216. <https://doi.org/10.32615/ps.2019.019>
- Razzaq AR, Ammara HM, Jhanab T, Mahmood A, Hafeez S, Hussain S (2016) A novel nanomaterial to enhance growth and yield of wheat. J Nanosci Technol 2:55–58. ISSN: 2455-0191
- Sabelli PA (2012) Seed development: a comparative overview on biology of morphology, physiology, and biochemistry between monocot and dicot plants. In: Agrawal G, Rakwal R (eds) Seed development: OMICS technologies toward improvement of seed quality and crop yield. Springer, Dordrecht. https://doi.org/10.1007/978-94-007-4749-4_1
- Salama H (2012) Effects of silver nanoparticles in some crop plants, common bean (*Phaseolus vulgaris* L.) and corn (*Zea mays* L.). Int Res J Biotechnol 3:190–197. ISSN: 2141-5153
- Scarpella E, Meijer AH (2004) Pattern formation in the vascular system of monocot and dicot plant species. New Phytol 164:209–242. <https://doi.org/10.1111/j.1469-8137.2004.01191.x>
- Scherer MD, Sposito JCV, Falco WF, Grisolia AB, Andrade LHC, Lima SM, Machado G, Nascimento VA, Goncalves DA, Wender H, Oliveira SL, Caires ARL (2019) Cytotoxic and genotoxic effects of silver nanoparticles on meristematic cells of *Allium cepa* roots: a close analysis of particle size dependence. Sci Total Environ 660:459–467. <https://doi.org/10.1016/j.scitotenv.2018.12.444>
- Shukla P, Chaurasia P, Younis K, Qadri OS, Faridi SA, Srivastava G (2019) Nanotechnology in sustainable agriculture: studies from seed priming to post-harvest management. Nanotechnol Environ Eng 4:11. <https://doi.org/10.1007/s41204-019-0058-2>
- Siddiqi KS, Husen A (2017) Plant response to engineered metal oxide nanoparticles. Nanoscale Res Lett 12:92. <https://doi.org/10.1186/s11671-017-1861-y>
- Silva T, Pokhrel LR, Dubey B, Tolaymat TM, Maier KJ, Liu X (2014) Particle size, surface charge and concentration dependent ecotoxicity of three organo-coated silver nanoparticles: comparison between general linear model-predicted and observed toxicity. Sci Total Environ 468–469:968–976. <https://doi.org/10.1016/j.scitotenv.2013.09.006>
- Soltis PS, Soltis DE (2016) Ancient WGD events as drivers of key innovations in angiosperms. Curr Opin Plant Biol 30:159–165. <https://doi.org/10.1016/j.pbi.2016.03.015>
- Spielman-Sun E, Lombi E, Donner E, Howard DL, Unrine JM, Lowry GV (2017) Impact of surface charge on cerium oxide nanoparticle uptake and translocation by wheat (*Triticum aestivum*). Environ Sci Technol 51:7361–7368. <https://doi.org/10.1021/acs.est.7b00813>
- Spielman-Sun E, Avellan A, Bland GD, Tappero RV, Acerbo AS, Unrine JM, Giraldo JP, Lowry GV (2019) Nanoparticle surface charge influences translocation and leaf distribution in vascular plants with contrasting anatomy. Environ Sci Nano 6:2508–2519. <https://doi.org/10.1039/C9EN00626E>
- Strasser RJ, Srivastava A, Tsimilli-Michael M (2000) The fluorescence transient as a tool to characterise and screen photosynthetic samples. In: Yunus M, Pathre U, Mohanty P (eds) Probing photosynthesis: mechanisms, regulation & adaptation. Taylor & Francis, London, pp 445–483
- Sukhanova A, Bozrova S, Sokolov P, Berestovoy M, Karaulov A, Nabiev I (2018) Dependence of nanoparticle toxicity on their physical and chemical properties. Nanoscale Res Lett 13:44. <https://doi.org/10.1186/s11671-018-2457-x>
- Tangaa SR, Selck H, Winther-Nielsen N, Khan FR (2016) Trophic transfer of metal-based nanoparticles in aquatic environments: a review and recommendations for future research focus. Environ Sci Nano 3:966–981. <https://doi.org/10.1039/C5EN00280J>
- Tolaymat TM, El Badawy AM, Genaidy A, Scheckel KG, Luxton TP, Suidan M (2010) An evidence-based environmental perspective of manufactured silver nanoparticle in syntheses and applications: a systematic review and critical appraisal of peer-reviewed scientific papers. Sci Total Environ 408:999–1006. <https://doi.org/10.1016/j.scitotenv.2009.11.003>
- Tripathi DK, Singh S, Singh S, Pandey R, Singh VP, Sharma NC, Prasad SM, Dubey NK, Chauhan DK (2017) An overview on manufactured nanoparticles in plants: uptake, translocation, accumulation and phytotoxicity. Plant Physiol Biochem 110:2–12. <https://doi.org/10.1016/j.plaphy.2016.07.030>
- Uzilday B, Turkan I, Ozgur R, Sekmen AH (2014) Strategies of ROS regulation and antioxidant defense during transition from C-3 to C-4 photosynthesis in the genus *Flaveria* under PEG-induced osmotic stress. J Plant Physiol 171:65–75. <https://doi.org/10.1016/j.jplph.2014.05.002>
- Vannini C, Domingo G, Onelli E, De Mattia F, Bruni I, Marsoni M, Bracale M (2014) Phytotoxic and genotoxic effects of silver nanoparticles exposure on germinating wheat seedlings. J Plant Physiol 171:1142–1148. <https://doi.org/10.1016/j.jplph.2014.05.002>
- Vinković T, Novák O, Strnad M, Goessler W, Jurašin DD, Parađiković N, Vrček IV (2017) Cytokinin response in pepper plants (*Cap-sicum annuum* L.) exposed to silver nanoparticles. Environ Res 156:10–18. <https://doi.org/10.1016/j.envres.2017.03.015>
- Wang S, Wu BD, Wei M, Zhou JW, Jiang K, Wang CY (2020) Silver nanoparticles with different concentrations and particle sizes affect the functional traits of wheat. Biol Plant 64:1–8. <https://doi.org/10.32615/bp.2019.122>
- Yan A, Chen Z (2019) Impacts of silver nanoparticles on plants: a focus on the phytotoxicity and underlying mechanism. Int J Mol Sci 20:1003. <https://doi.org/10.3390/ijms20051003>

- Yang J, Jiang F, Ma C, Rui YK, Rui M, Muhammad A, Cao W, Xing B (2018) Alteration of crop yield and quality of wheat upon exposure to silver nanoparticles in a life cycle study. *J Agric Food Chem* 66:2589–2597. <https://doi.org/10.1021/acs.jafc.7b04904>
- Yang L, Su D, Chang X, Foster CSP, Sun L, Huang CH, Zhou X, Zeng L, Ma H, Zhong B (2020) Phylogenomic insights into deep phylogeny of angiosperms based on broad nuclear gene sampling. *Plant Commun* 1:100027. <https://doi.org/10.1016/j.xplc.2020.100027>
- Ye ZP, Ling Y, Yu Q, Duan HL, Kang HJ, Huang GM, Duan SH, Chen XM, Liu YG, Zhou SX (2020) Quantifying light response of leaf-scale water-use efficiency and its interrelationships with photosynthesis and stomatal conductance in C₃ and C₄ species. *Front Plant Sci* 11:374. <https://doi.org/10.3389/fpls.2020.00374>
- Yin LY, Cheng YW, Espinasse B, Colman BP, Auffan M, Wiesner M, Rose J, Liu J, Bernhardt ES (2011) More than the ions: the effects of silver nanoparticles on *Lolium multiflorum*. *Environ Sci Technol* 45:2360–2367. <https://doi.org/10.1021/es103995x>
- Zhao X, Han L, Xiao J, Wang L, Liang T, Liao X (2020) A comparative study of the physiological and biochemical properties of tomato (*Lycopersicon esculentum* M.) and maize (*Zea mays* L.) under palladium stress. *Sci Total Environ* 705:135938. <https://doi.org/10.1016/j.scitotenv.2019.135938>
- Zhu ZJ, Wang H, Yan B, Zheng H, Jiang Y, Miranda OR, Rotello VM, Xing B, Vachet RW (2012) Effect of surface charge on the uptake and distribution of gold nanoparticles in four plant species. *Environ Sci Technol* 46:12391–12398. <https://doi.org/10.1021/es301977w>
- Zuverza-Mena N, Armendariz R, Peralta-Videa JR, Gardea-Torresdey JL (2016) Effects of silver nanoparticles on radish sprouts: root growth reduction and modifications in the nutritional value. *Front Plant Sci* 7:90. <https://doi.org/10.3389/fpls.2016.00090>

Publisher's Note Springer Nature remains neutral with regard to jurisdictional claims in published maps and institutional affiliations.

Authors and Affiliations

Ewelina Matras¹  · Anna Gorczyca¹  · Ewa Pociecha²  · Sebastian Wojciech Przemieniecki³  · Magdalena Oćwieja⁴ 

Anna Gorczyca
anna.gorczyca@urk.edu.pl

Ewa Pociecha
ewa.pociecha@urk.edu.pl

Sebastian Wojciech Przemieniecki
sebastian.przemieniecki@uwm.edu.pl

Magdalena Oćwieja
magdalena.ocwieja@ikifp.edu.pl

¹ Department of Microbiology and Biomonitoring, Faculty of Agriculture and Economics, University of Agriculture in Krakow, Mickiewicz Ave. 21, 31-120 Krakow, Poland

² Department of Plant Breeding, Physiology and Seed Science, Faculty of Agriculture and Economics, University of Agriculture in Krakow, Podłużna 3, 30-239 Krakow, Poland

³ Department of Entomology, Phytopathology and Molecular Diagnostics, University of Warmia and Mazury, Prawocheńskiego 17, 10-720 Olsztyn, Poland

⁴ Jerzy Haber Institute of Catalysis and Surface Chemistry, Polish Academy of Sciences, Niezapominajek 8, 30-239 Krakow, Poland